IEEE Access
Multidisciplinary | Rapid Review | Open Access Journal

Received 9 October 2022, accepted 25 October 2022, date of publication 1 November 2022, date of current version 9 November 2022.

Digital Object Identifier 10.1109/ACCESS.2022.3218657

RESEARCH ARTICLE

State-Space PID: A Missing Link Between Classical and Modern Control

WEN TAN[1], (Member, IEEE), WENJIE HAN[2], AND JIAOHU XU[2]
[1]School of Electrical and Control Engineering, North China University of Technology, Beijing 100144, China
[2]School of Control and Computer Engineering, North China Electric Power University, Beijing 102206, China

Corresponding author: Wen Tan (wtan@ieee.org)

ABSTRACT PID control is widely applied in industry. However, it is classified as a classical control technique, in that transfer function method is used to represent the ideal and/or practical PID controller. Modern control concepts, such as state feedback, observer, are seldom found in PID research. This paper proposes a state-space PID structure to fill the gap. The classical ideal PID is first shown to be a state-feedback control structure with the plant output and its derivative and integral as the states, and then a model-independent observer is proposed to estimate the states, thus approximate the ideal PID as an observer-based state feedback control structure (state-space PID). Then it is shown that the proposed state-space PID structure is the dual of the linear active disturbance rejection control structure, and it is a general-purposed control structure in that any strictly-proper linear controller with integration can be implemented via the proposed structure. The design of the state-space PID can be done via the well-known pole placement algorithm in modern control. Simulation and experiment results show that state-space PID structure is a practical implementation of ideal PID, which naturally integrates the noise reduction that is separated from PID tuning, and it is a natural generalization of the classical PID to high-order cases.

INDEX TERMS PID control, control structure, observer, active disturbance rejection control, pole placement.

I. INTRODUCTION

Proportional-Integral-Derivative (PID) loops are by far the most common feedback control mechanism for industrial processes [1], [2], [3]. The three parameters of a PID controller have a very clear connection with the performance of the system, so it can be easily tuned online. However, with the increasing complexity of industrial processes and the increase of various uncertainties in the plants, the control performance of classical PID control may not be satisfactory due to its specific structure [4].

On the other hand, many modern control techniques were tried to replace the PID control, e.g., LQG [5], H_∞ [6], adaptive control [7]. Although the advanced control techniques have contributed to the improvement of the control performance, they are seldom found in practice due to the implementation, tuning and maintenance issues. When a process is already up and running, the trial-and-error design can be more convenient than the advanced control alternatives that require taking the process offline for tests. And even when the advanced control technique theoretically would provide improved performance, the extra effort and expense required may not be worth it. Therefore, more than 90% of the controllers in feedback control are still of PID type [1], [8].

PID control has been investigated thoroughly in the past. The first practical PID controller tuning method was proposed by Ziegler-Nichols [9]. Since then, hundreds of PID tuning methods have been proposed, e.g., gain-phase margin [10], [11]; internal model control (IMC) [12], [13], [14]; stabilizing parameter space [15]; direct synthesis [16], [17]; relay feedback [18]; see [19] for a recent review of PID tuning methods.

The tuning of PID controllers are most based on the ideal PID structure. However, due to the measurement noise, the ideal PID cannot be directly used in practice, and filters have to be added to reduce the effect of noise, thus additional filter constant has to be tuned together with the

The associate editor coordinating the review of this manuscript and approving it for publication was Qi Zhou.

PID parameters, which makes the tuning of PID more complex [20]. Though filters are very important for PID control, there are not many references on the tuning of the PID filters. Reference [21], [22] considered measurement noise filtering for common PID tuning rules; [23], [24] discussed the optimization of PID controller with noise filter.

It is well-known that PID control is a restricted-structure controller, which has a second-order transfer function with special structure. High-order PID are proposed to improve the performance of the classical PID. A PID+lead structure was proposed in [25] and it was shown that the structure is effective for unstable process with time delay [26], [27]. PID plus second-order derivative controller ($PIDD^2$) was applied in automatic regulator system and its effectiveness over classical PID was shown. Fractional-order PID (FOPID) is in fact a high-order PID form that was used to improve the performance of the classical PID [28], [29].

It is strange to note that although modern control has been developed since 1970s, PID is seldom tuned in the state-space framework. The main problem is that a PID controller is a fixed control structure with derivative of the plant output. If it is to be realized in the state space, it is of a special control structure and generally has a smaller order than the controlled plant, thus designing a PID controller in state space amounts to finding the parameters for a fixed-order controller. The design can be solved with numerical method such as linear matrix inequality (LMI) [30], [31] but the essential tools in modern control such as state feedback and observer are lost.

Recently, active disturbance rejection control (ADRC) technique was proposed in [32]. ADRC treats the controlled plant as a cascaded integral model, and lumps all the model uncertainties and external disturbances into a single disturbance (called total disturbance in ADRC framework). An extended state observer (ESO) is used to estimate the total disturbance, and the estimated disturbance is rejected via a state-feedback control law. ADRC does not rely on the plant model, and the linear version of ADRC (LADRC) can be tuned via the bandwidth idea [33], [34], thus LADRC is a potential control structure to replace PID in practice. It was shown that a second-order LADRC is a PID+filter structure [35], and the PID parameters can be converted from second-order LADRC [36], [37]. It is also found that the well-known Ziegler-Nichols tuning for PID controller can be interpreted in ADRC framework [38] via the disturbance-rejection PID idea. However, as a disturbance observer based control (DOBC) method [39], the control structure is different from the classical PID form, and most of the control engineers are not familiar with the design and tuning idea.

This paper proposes an implementation of the classical PID with a state-space structure. The state-space PID (SS-PID) has the same structure as the classical PID with the derivative of the plant output estimated via a model-independent observer, thus retains the model-independence property of the classical PID. The idea is then extended to high-order case and the relation with LADRC is investigated. It is also proved that the state-space PID is a general-purposed control structure in that any linear finite-dimensional strictly-proper controller with integration can be implemented with the structure. A state-space pole placement method is proposed to design (high-order) PID controller, and the state-space PID structure can thus be tuned with two parameters. Simulation examples and experiment results show that the state-space PID can achieve better performance for some complex systems than the classical PID.

The main contributions of the paper can be summarized as follows:

1) A state-space PID structure is proposed so that PID controller can be expressed in the state-space form. The output and its derivative are estimated with a cascaded integral model instead of the true plant model, thus the state-space PID retains the structure independence on the plant as the classical PID.
2) The state-space PID structure is shown to be the dual of the LADRC structure when the observer (controller) gain of the SS-PID is chosen as the transpose of the controller (observer) gain of the LADRC, which reveals the fact that SS-PID and LADRC are using the same canonical model as the controlled plant but design via different viewpoints.
3) The state-space PID is shown to be a general-purposed control structure in that any finite-dimensional strictly-proper linear controller with integration can be implemented with the structure, thus removes the structural limitations of classical PID.
4) A pole placement method is proposed to design (high-order) PID control and the state-space PID can be tuned via two parameters. It is also demonstrated that higher-order state-space PID can achieve better control performance than the classical PID, thus higher-order PID can be used to improve the control performance for complex systems.

The rest of the paper is arranged as follows: Section 2 proposes a state-space PID implementation of the ideal PID controller, and extends it to high-order PID in Section 3. The relation between the state-space PID structure and the LADRC structure is discussed in Section 4. Then the generality of state-space PID structure is proved in Section 5. Section 6 proposes a PID design method via the state-feedback pole-placement idea. Section 7 verifies the proposed structure on a temperature control lab. Finally conclusions are given in Section 8. All the simulations are performed in MATLAB/SIMULINK with variable-step ODE45(Dormand Prince) method, and the experiment is performed with fixed-step ODE4(Runger-Kutta) method with sampling time 0.5 second.

II. STATE-SPACE FORM OF PID

PID controllers are widely used in industry due to its simple structure and easy tuning procedure. An ideal PID controller

has the following transfer function:

$$K_{PID}(s) = K_p + \frac{K_i}{s} + K_d s \tag{1}$$

where K_p, K_i, K_d are the proportional, integral, and derivative gain, respectively. PID control can be written as a state-feedback control law:

$$\begin{aligned} u(t) &= K_d(\dot{r}(t) - \dot{y}(t)) + K_p(r(t) - y(t)) \\ &\quad + K_i \int_0^t (r(\tau) - y(\tau))d\tau \\ &=: \bar{K}_o(\bar{r}(t) - x(t)) \end{aligned} \tag{2}$$

where $y(t)$ is the controlled variable, $u(t)$ is the manipulated variable, and $r(t)$ is the reference signal,

$$\bar{r}(t) = [\dot{r}(t) \;\; r(t) \;\; \int_0^t r(\tau)d\tau]^T \tag{3}$$

and the state vector is

$$x(t) = [\dot{y}(t) \;\; y(t) \;\; \int_0^t y(\tau)d\tau]^T \tag{4}$$

with state-feedback gain

$$\bar{K}_o = [K_d \;\; K_p \;\; K_i] \tag{5}$$

In practice $\dot{y}(t)$ is usually computed from $y(t)$ via a practical differentiator. An alternative method to obtain the derivative of $y(t)$ is to estimate it with an observer. Consider the following double integral system:

$$\ddot{y}(t) = u(t) \tag{6}$$

Let

$$x_1 = \dot{y}, \quad x_2 = y \tag{7}$$

then it can be written in the state-space form:

$$\begin{cases} \begin{bmatrix} \dot{x}_1 \\ \dot{x}_2 \end{bmatrix} = \bar{A} \begin{bmatrix} x_1 \\ x_2 \end{bmatrix} + \bar{B}u \\ y = \bar{C} \begin{bmatrix} x_1 \\ x_2 \end{bmatrix} \end{cases} \tag{8}$$

where

$$\bar{A} = \begin{bmatrix} 0 & 0 \\ 1 & 0 \end{bmatrix}, \quad \bar{B} = \begin{bmatrix} 1 \\ 0 \end{bmatrix}, \; \bar{C} = \begin{bmatrix} 0 & 1 \end{bmatrix} \tag{9}$$

thus the following observer can be used to estimate $[\dot{y} \;\; y]^T$.

$$\begin{bmatrix} \dot{\bar{x}}_1 \\ \dot{\bar{x}}_2 \end{bmatrix} = (\bar{A} - \bar{L}\bar{C}) \begin{bmatrix} \bar{x}_1 \\ \bar{x}_2 \end{bmatrix} + \bar{B}u + \bar{L}y \tag{10}$$

where $\bar{L}$ is the observer gain

$$\bar{L} = [\bar{\beta}_1 \;\; \bar{\beta}_2]^T \tag{11}$$

If $\bar{L}$ is chosen such that $\bar{A} - \bar{L}\bar{C}$ is asymptotically stable, then $\bar{x}_1 \to \dot{y}$ and $\bar{x}_2 \to y$.

Define a new state $\bar{x}_3$, where

$$\dot{\bar{x}}_3 = \bar{x}_2 \tag{12}$$

Since $\bar{x}_2 \to y$, we have $\bar{x}_3 \to \int_0^t y(\tau)d\tau$ when $\bar{A} - \bar{L}\bar{C}$ is asymptotically stable.

Combine (10) and (12), we have an estimation of the state (4) with the following extended state observer:

$$\dot{\bar{x}} = (\bar{A}_e - \bar{L}_o\bar{C}_e)\bar{x} + \bar{B}_e u + \bar{L}_o y \tag{13}$$

where

$$\bar{x} = [\bar{x}_1 \;\; \bar{x}_2 \;\; \bar{x}_3]^T \tag{14}$$

is the estimated state vector,

$$\bar{A}_e = \begin{bmatrix} 0 & 0 & 0 \\ 1 & 0 & 0 \\ 0 & 1 & 0 \end{bmatrix}, \quad \bar{B}_e = \begin{bmatrix} 1 \\ 0 \\ 0 \end{bmatrix}, \; \bar{C}_e = \begin{bmatrix} 0 & 1 & 0 \end{bmatrix} \tag{15}$$

and

$$\bar{L}_o = [\bar{L} \;\; 1]^T = [\bar{\beta}_1 \;\; \bar{\beta}_2 \;\; 1]^T \tag{16}$$

is the observer gain.

So an ideal PID controller can be implemented with the the following state-space controller.

$$\begin{cases} \dot{\bar{x}} = (\bar{A}_e - \bar{L}_o\bar{C}_e)\bar{x} + \bar{B}_e u + \bar{L}_o y \\ u = \bar{K}_o(\bar{r} - \bar{x}) \end{cases} \tag{17}$$

Its structure is shown in Figure 1.

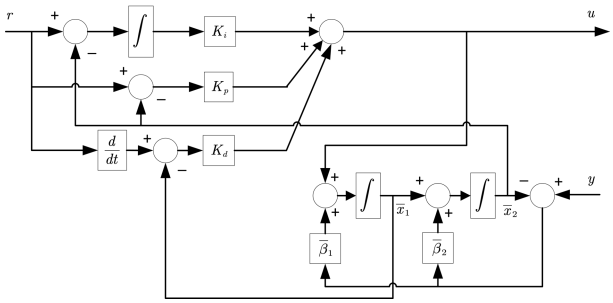

FIGURE 1. Block diagram of state-space PID.

Remark 1: It is noted that the state $x(t)$ (4) is estimated using the system (6) instead of using the true model of the controlled plant. The idea is similar to high-gain observers [40] and extended state observers [32], [34]. Of course, the plant model can be used in estimating the state $x(t)$ [41], [42], however, if the plant model is used, then the resulting PID will depend on it, and the model-independence property of the PID control structure will be lost.

It is easy to show that the state-space PID (17) is equivalent to the control structure shown in Figure 2, where the setpoint filter is

$$C_1(s) = (1 - \bar{K}_o(sI - \bar{A}_e + \bar{B}_e\bar{K}_o + \bar{L}_o\bar{C}_e)^{-1}\bar{B}_e)F_r(s) \tag{18}$$

where $F_r(s)$ is the transfer function from the reference $r(t)$ to the extended reference $\bar{r}(t)$ (3), so

$$F_r(s) = \bar{K}_o[s \;\; 1 \;\; \frac{1}{s}]^T = \frac{K_d s^2 + K_p s + K_i}{s} \tag{19}$$

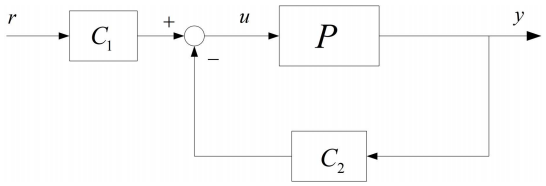

FIGURE 2. Feedback control structure with setpoint filter.

and the feedback controller is

$$C_2(s) = \bar{K}_o(sI - \bar{A}_e + \bar{B}_e\bar{K}_o + \bar{L}_o\bar{C}_e)^{-1}\bar{L}_o \tag{20}$$

It is clear that the internal stability, robustness, and the disturbance-rejection performance of the structure is only related to the feedback controller $C_2(s)$.

To show that the state-space PID is an approximation of the ideal PID, consider the feedback controller $C_2(s)$ of the state-space PID (17), which has the the following transfer function from y to u:

$$\frac{(K_d\bar{\beta}_1 + K_p\bar{\beta}_2 + K_i)s^2 + (K_p\bar{\beta}_1 + K_i\bar{\beta}_2)s + K_i\bar{\beta}_1}{s[s^2 + (K_d + \bar{\beta}_2)s + (\bar{\beta}_1 + K_d\bar{\beta}_2 + K_p)]} \tag{21}$$

Divide both the numerator and the denominator of the transfer function (21) by $\bar{\beta}_1$, it can be concluded that if

$$\bar{\beta}_1 \gg 1, \quad \frac{\bar{\beta}_2}{\bar{\beta}_1} \ll 1 \tag{22}$$

then $C_2(s)$ of the state-space PID (17) will approximate the ideal PID (1).

In practice, an ideal PID is implemented as the following practical PID controller:

$$K_c(s) = K_p(1 + \frac{1}{T_i s} + \frac{T_d s}{T_d/Ns + 1}) \tag{23}$$

where $T_i = \frac{K_p}{K_i}$ is the integration time constant and $T_d = \frac{K_d}{K_p}$ is the derivative time constant. N is the filter constant to attenuate the high-frequency noise in the derivative. It can be shown that if

$$\bar{\beta}_1 \gg 1, \quad \frac{\bar{\beta}_2}{\bar{\beta}_1} = \frac{T_d}{N} \tag{24}$$

then the feedback controller $C_2(s)$ of the state-space PID (17) will approximate the practical PID (23).

For simplicity, the observer gain $\bar{L}$ (11) can be tuned via the bandwidth idea, i.e., the poles of $\bar{A} - \bar{L}\bar{C}$ in (10) are placed at the same location $-\bar{\omega}_o$, then

$$\bar{\beta}_1 = \bar{\omega}_o^2, \quad \bar{\beta}_2 = 2\bar{\omega}_o \tag{25}$$

so the observer gain $\bar{L}_o$ for the state-space PID (17) is

$$\bar{L}_o = [\bar{\omega}_o^2 \;\; 2\bar{\omega}_o \;\; 1]^T \tag{26}$$

thus when $\bar{\omega}_o$ is large enough, the feedback controller $C_2(s)$ of the state-space PID (17) will approximate the ideal PID (1), and when $\bar{\omega}_o = 2N/T_d$, it will approximate the practical PID (23).

It can be shown from (21) that the state-space PID (17) is like an ideal PID cascaded with a second-order filter. The filter introduces roll-off at high frequencies thus reduces the sensitivity to measurement noise. So state-space PID is a practical implementation of ideal PID. It is an observer-based state feedback controller that has a special state-space (cascaded integral) model. So it has a fixed control structure as the ideal PID but with a model-independent observer to estimate the derivative and integral of the controlled variable.

Example 1: Consider a first-order plus deadtime (FOPDT) process

$$P_1(s) = \frac{1}{s+1}e^{-0.4s} \tag{27}$$

The parameters of an ideal PID controller tuned by AMIGO method [43] is:

$$K_p = 1.325, \quad T_i = 0.768, \; T_d = 0.1786 \tag{28}$$

The response of the process under the ideal PID is shown in Figure 3(a) when a unit step reference signal is inserted at $t = 1$s and a unit step input disturbance is inserted at $t = 10$s, together with the responses of the practical PID with $N = 20$ and the state-space PID (17) with $\bar{\omega}_o = 40/T_d$.

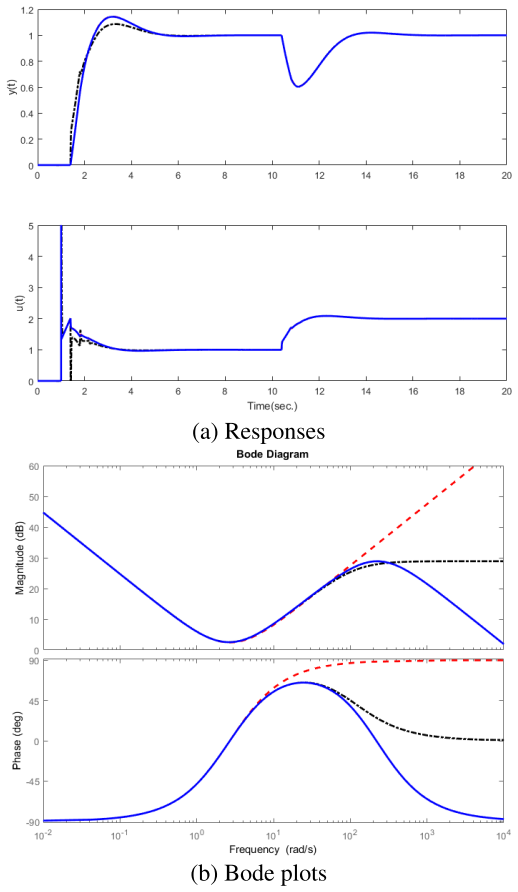

(a) Responses

(b) Bode plots

FIGURE 3. Responses and bode plots of various PID for Example 1 (solid: state-space PID; dashed: ideal PID; dashdotted: practical PID).

The response of the state-space PID is very close (indistinguishable in the figure) to the ideal PID for both setpoint and disturbance responses. (Figure 3(a) only shows the controller output $u(t)$ within the range from 0 to 5, otherwise $u(t)$ for the disturbance response will be too small to be visible in the figure).

The Bode plots for the ideal PID, the practical PID ($N = 20$), the feedback controllers $C_2(s)$ of the state-space PID ($\bar{\omega}_o = 40/T_d$) are shown in Figure 3(b). It is clear that the three controllers differ only at high frequencies and only the state-space PID rolls off at high frequencies, thus the state-space PID has the best noise attenuation performance. For example, suppose there is a white noise with variance 0.001 added to the output of the plant, the variances of the output for the state-space PID, the ideal PID, and the practical PID are 0.1061, 0.2015, and 0.1076, respectively, which verifies the claim from the Bode plots.

III. HIGH-ORDER EXTENSION

The state-space PID idea can be easily extended to higher-order case, thus it extends the classical PID control and is applicable for complex systems where high-order derivatives of the plant output are needed to improve the control performance.

The pth-order state-space PID (SS-PID) has the form:

$$\begin{cases} \dot{\bar{x}} = (\bar{A}_e - \bar{L}_o\bar{C}_e)\bar{x} + \bar{B}_e u + \bar{L}_o y \\ u = \bar{K}_o(\dfrac{1}{b_0}\bar{r} - \bar{x}) \end{cases} \tag{29}$$

where the state vector is defined as

$$\bar{x} = [\bar{x}_1 \;\; \bar{x}_2 \;\; \cdots \;\; \bar{x}_p \;\; \bar{x}_{p+1}]^T \tag{30}$$

and the state-space data are

$$\bar{A}_e = \begin{bmatrix} 0 & 0 & \cdots & 0 & 0 \\ 1 & 0 & \cdots & 0 & 0 \\ 0 & 1 & \cdots & 0 & 0 \\ \vdots & \vdots & \ddots & \vdots & \vdots \\ 0 & 0 & \cdots & 1 & 0 \end{bmatrix}_{(p+1)\times(p+1)}, \quad \bar{B}_e = \begin{bmatrix} 1 \\ 0 \\ 0 \\ \vdots \\ 0 \end{bmatrix}_{(p+1)\times 1},$$
$$\bar{C}_e = \begin{bmatrix} 0 & \cdots & 0 & b_0 & 0 \end{bmatrix}_{1\times(p+1)} \tag{31}$$

It is clear that the state-space PID can be regarded as an observer-based state feedback control for the following extended system (where $\bar{A}_e, \bar{B}_e, \bar{C}_e$ are given in (31))

$$\begin{cases} \dot{x} = \bar{A}_e x + \bar{B}_e u \\ y = \bar{C}_e x \end{cases} \tag{32}$$

with the observer gain $\bar{L}_o$, where

$$\bar{L}_o = [\bar{\beta}_1 \;\; \bar{\beta}_2 \;\; \cdots \;\; \bar{\beta}_p \;\; 1]^T/b_0 \tag{33}$$

and the controller gain $\bar{K}_o$, where

$$\bar{K}_o = [\bar{k}_1 \;\; \bar{k}_2 \;\; \cdots \;\; \bar{k}_p \;\; \bar{k}_{p+1}] \tag{34}$$

It is clear that the states and the output of the extended model (32) are related by:

$$\begin{aligned} &\dot{x}_1(t) = u(t), \quad \dot{x}_2(t) = x_1(t), \cdots, \dot{x}_p(t) = x_{p-1}(t), \\ &\dot{x}_{p+1}(t) = x_p(t), \quad y(t) = b_0 x_p(t) \end{aligned} \tag{35}$$

So $x_i(t)(i = 1, \cdots, p)$ have clear physical meaning, i.e.,

$$x_p(t) = \frac{1}{b_0}y(t), \quad x_{p-1}(t) = \frac{1}{b_0}\dot{y}(t), \cdots, x_1(t) = \frac{1}{b_0}y^{(p-1)}(t) \tag{36}$$

and

$$x_{p+1}(t) = \int_0^t x_p(\tau)d\tau = \frac{1}{b_0}\int_0^t y(\tau)d\tau \tag{37}$$

thus $x(t)$ is composed of $y(t)$, its integral and its derivatives of various order divided by b_0.

When $\bar{L}_o$ is chosen properly, $\bar{A}_e - \bar{L}_o\bar{C}_e$ is asymptotically stable, we have

$$\begin{aligned} &\bar{x}_1(t) \to \frac{1}{b_0}y^{(p-1)}(t), \cdots, \bar{x}_p(t) \to \frac{1}{b_0}y(t), \\ &\bar{x}_{p+1}(t) \to \frac{1}{b_0}\int_0^t y(\tau)d\tau \end{aligned} \tag{38}$$

so the elements $\frac{\bar{k}_{p-j}}{b_0}(j = 0, 1, \cdots, p-1)$ are the gains of the jth-order derivative of $y(t)$, and $\frac{\bar{k}_{p+1}}{b_0}$ is the gain of the integral of $y(t)$, thus the pth-order state-space PID is a practical implementation of high-order PID

$$K(s) = K_p + \frac{K_i}{s} + K_{d1}s + K_{d2}s^2 + \cdots + K_{d,p-1}s^{p-1} \tag{39}$$

with gains

$$\begin{aligned} &K_p = \bar{k}_p/b_0, \quad K_i = \bar{k}_{p+1}/b_0, \\ &K_{dj} = \bar{k}_{p-j}/b_0, \quad (j = 1, 2, \cdots, p-1) \end{aligned} \tag{40}$$

In other words, the state-feedback gain of the pth-order SS-PID is related to the gains of the high-order PID (39) by

$$\bar{K}_o = [K_{d,p-1} \;\; \cdots \;\; K_{d2} \;\; K_d \;\; K_p \;\; K_i]b_0 \tag{41}$$

Remark 2: The transfer function of the extended system (32) is

$$y^{(p)}(t) = b_0 u(t) \tag{42}$$

thus for the pth-order state-space PID, the output $y(t)$ and its derivatives are estimated from the cascaded integral model (42) instead of the true plant model. Thus model-independent control structure of PID is retained.

Remark 3: b_0 is a parameter that scales the estimation of the output y. Its effect is to change the overall controller gain. This can be verified by the transfer function from y to u of the state-space PID. For example, when $p = 2$, the feedback controller from y to u becomes

$$\frac{(\bar{k}_1\bar{\beta}_1 + \bar{k}_2\bar{\beta}_2 + \bar{k}_3)s^2 + (\bar{k}_2\bar{\beta}_1 + \bar{k}_3\bar{\beta}_2)s + \bar{k}_3\bar{\beta}_1}{b_0 s[s^2 + (\bar{k}_1 + \bar{\beta}_2)s + (\bar{\beta}_1 + \bar{k}_1\bar{\beta}_2 + \bar{k}_2)]} \tag{43}$$

When $\bar{k}_1, \bar{k}_2, \bar{k}_3$ and $\bar{\beta}_2, \bar{\beta}_2$ are fixed, $1/b_0$ varies the gain of the controller.

Remark 4: To approximate the ideal PID controller (1) with gains K_p, K_i, and K_d, the controller gain of the second-order SS-PID can be chosen as

$$\bar{K}_o = [K_d \;\; K_p \;\; K_i]b_0 \tag{44}$$

then the transfer function from y to u of the second-order state-space PID becomes

$$\frac{(K_d\bar{\beta}_1 + K_p\bar{\beta}_2 + K_i)s^2 + (K_p\bar{\beta}_1 + K_i\bar{\beta}_2)s + K_i\bar{\beta}_1}{s[s^2 + (K_d b_0 + \bar{\beta}_2)s + (\bar{\beta}_1 + K_p b_0 + K_d b_0\bar{\beta}_2)]} \tag{45}$$

In this case b_0 can be set to a small value so that the second-order SS-PID can approximate the ideal PID with a small observer bandwidth, which is useful since the observer bandwidth should not be too large in practice under noisy environment.

The diagram of the pth-order state-space PID (SS-PID) is shown in Figure 4, where the derivatives of the signal r are set to zero for step-like reference, and α is a setpoint weight to reduce the overshoot when necessary (e.g., for integrating and unstable processes). By default $\alpha = 1$.

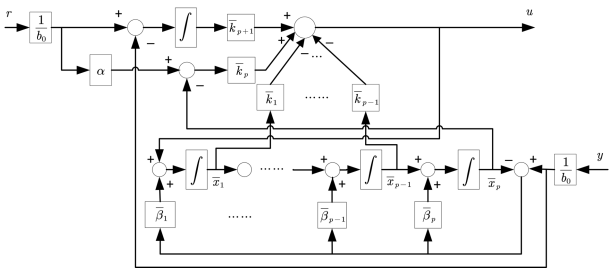

FIGURE 4. Block diagram of *p*th-order state-space PID.

IV. RELATION WITH ADRC

Consider the dual system of (32), i.e.,

$$\begin{cases} \dot{z} = \hat{A}_e z + \hat{B}_e u \\ y = \hat{C}_e z \end{cases} \tag{46}$$

where $z = [z_1 \;\; \cdots \;\; z_p \;\; z_{p+1}]^T$ is the state vector, and

$$\begin{aligned} \hat{A}_e &= \bar{A}_e^T = \begin{bmatrix} 0 & 1 & 0 & \cdots & 0 \\ 0 & 0 & 1 & \cdots & 0 \\ \vdots & \vdots & \vdots & \ddots & \vdots \\ 0 & 0 & 0 & \cdots & 1 \\ 0 & 0 & 0 & \cdots & 0 \end{bmatrix}_{(p+1)\times(p+1)}, \\ \hat{B}_e &= \bar{C}_e^T = [0 \;\; \cdots \;\; 0 \;\; b_0 \;\; 0]^T_{(p+1)\times 1}, \\ \hat{C}_e &= \bar{B}_e^T = [1 \;\; 0 \;\; 0 \;\; \cdots \;\; 0]_{1\times(p+1)} \end{aligned} \tag{47}$$

We can construct an observer-based state-feedback controller for (46) as

$$\begin{cases} \dot{\hat{z}} = (\hat{A}_e - \hat{L}_o\hat{C}_e)\hat{z} + \hat{B}_e u + \hat{L}_o y \\ u = \hat{K}_o(\hat{r} - \hat{z}) \end{cases} \tag{48}$$

where the extended referece signal is

$$\hat{r}(t) = [r(t) \;\; \dot{r}(t) \;\; \cdots \;\; r^{(p)}(t) \;\; 0]^T \tag{49}$$

$\hat{K}_o$ is the controller gain vector,

$$\hat{K}_o = [\hat{k}_1 \;\; \hat{k}_2 \;\; \cdots \;\; \hat{k}_p \;\; 1]/b_0 \tag{50}$$

and $\hat{L}_o$ is the observer gain vector.

$$\hat{L}_o = [\hat{\beta}_1 \;\; \hat{\beta}_2 \;\; \cdots \;\; \hat{\beta}_p \;\; \hat{\beta}_{p+1}]^T \tag{51}$$

Compare (29) and (48), if

$$\hat{K}_o = \bar{L}_0^T, \quad \hat{L}_o = \bar{K}_o^T \tag{52}$$

then

$$\hat{A}_e - \hat{L}_o\hat{C}_e - \hat{B}_e\hat{K}_o = (\bar{A}_e - \bar{B}_e\bar{K}_o - \bar{L}_o\bar{C}_e)^T \tag{53}$$

thus (29) and (48) are dual systems if the reference signal is not considered. So the feedback controller of (48) is the transpose of the feedback controller of (29). As they are single-variable systems, *the feedback controller of* (48) *is exactly equal to the feedback controller of* (29).

It is noted that the observer-based state-feedback controller designed for the extended plant (46) is just the linear active disturbance rejection controller (LADRC) [44]. The idea of LADRC is to model the controlled plant as

$$y^{(p)}(t) = b_0 u(t) + f \tag{54}$$

where f is a combination of the unknown dynamics and the external disturbances of the plant, and denoted as the *total disturbance*. A linear extended state observer (ESO) is used to estimate the unknown total disturbance f and the derivatives of y, and the estimated disturbance is rejected with a linear state-feedback control law. The final pth-order LADRC has the same form as (48). The structure of a second-order LADRC is shown in Figure 5.

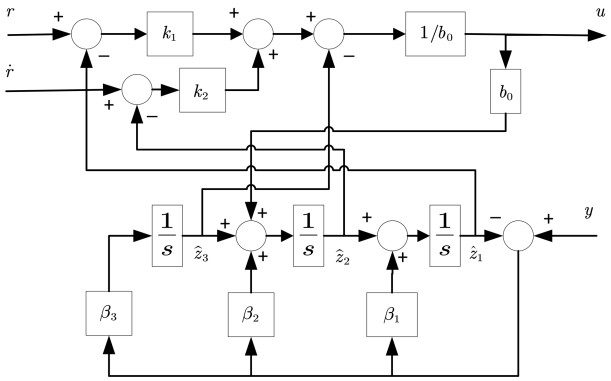

FIGURE 5. Block diagram of second-order LADRC.

When (52) holds, LADRC (48) is the dual of SS-PID (29) if reference signal is not considered, thus the feedback controller of LADRC (48) is equivalent to the feedback controller of SS-PID (29), thus it has the same disturbance rejection performance and robust stability as the SS-PID. However,

their setpoint responses are different since the setpoint filters are different, as is shown in the following example.

Example 2: (Continue from Example 1) The response of the closed-loop system for the controlled plant in Example 1 under a second-order LADRC with the following parameters is shown in Figure 6, together with the state-space PID in Example 1. It is shown that the disturbance response of the second-order LADRC is the same as that of the state-space PID but the setpoint response is different (Figure 6 shows only part of the controller output $u(t)$ of the second-order LADRC as its initial output is too large).

$$b_0 = 1, \quad K_o = [1600 \;\; 80 \;\; 1], \; L_o = [K_d \;\; K_p \;\; K_i]^T \quad (55)$$

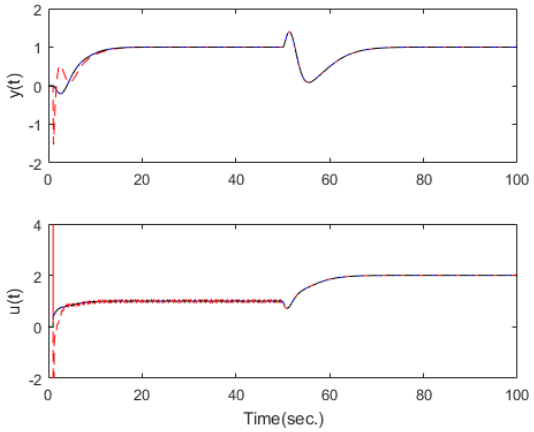

FIGURE 6. Responses for Example 2 (solid: state-space PID; dashed: second-order LADRC (55).

Remark 5: It is clear that both state-space PID and LADRC use the same model (42) in the design: LADRC extends the model with an observable state-space system (46) with the extended state treated as the total disturbance, while state-space PID extends the model with a controllable state-space system (32) with the extended state as the integral of the plant output. The final designed controllers are dual if reference tracking is not considered and the parameters are related as in (52).

V. GENERALITY OF STATE-SPACE PID

It is well-known that the classical PID controller is a restricted complexity controller and general linear controllers may have to be used to achieve better performance. In this section we will show that the state-space PID (29) can serve as a general-purposed linear control structure, i.e., for any $(p+1)$th-order linear finite-dimensional strictly-proper transfer function $K_c(s)$ with integration, we can always find the process gain b_0, the observer gain $\bar{L}_o$ (33), and the state-feedback gain $\bar{K}_o$ (34) so that the feedback controller of the pth-order SS-PID (29) is equal to $K_c(s)$, i.e.,

$$\bar{K}_o(sI - \bar{A}_e + \bar{B}_e\bar{K}_o + \bar{L}_o\bar{C}_e)^{-1}\bar{L}_o = K_c(s) \quad (56)$$

For the pth-order SS-PID (29), the transfer function of the feedback controller $C_2(s)$ is

$$C_2(s) = \frac{c_p s^p + c_{p-1}s^{p-1} + \cdots + c_0}{s^{p+1} + a_p s^p + \cdots + a_1 s} \quad (57)$$

where the numerator coefficients can be computed from

$$\begin{bmatrix} c_p \\ c_{p-1} \\ \vdots \\ c_1 \\ c_0 \end{bmatrix} = \frac{1}{b_0} \begin{bmatrix} \bar{\beta}_1 & \bar{\beta}_2 & \cdots & \bar{\beta}_p & 1 \\ 0 & \bar{\beta}_1 & \cdots & \bar{\beta}_{p-1} & \bar{\beta}_p \\ \vdots & \vdots & \ddots & \vdots & \vdots \\ 0 & 0 & \cdots & \bar{\beta}_1 & \bar{\beta}_2 \\ 0 & 0 & \cdots & 0 & \bar{\beta}_1 \end{bmatrix} \begin{bmatrix} \bar{k}_1 \\ \bar{k}_2 \\ \vdots \\ \bar{k}_p \\ \bar{k}_{p+1} \end{bmatrix} \quad (58)$$

and the denominator coefficients can be computed from

$$\begin{bmatrix} a_p \\ a_{p-1} \\ \vdots \\ a_2 \\ a_1 \end{bmatrix} = \begin{bmatrix} \bar{\beta}_p & 1 & 0 & \cdots & 0 & 0 \\ \bar{\beta}_{p-1} & \bar{\beta}_p & 1 & \cdots & 0 & 0 \\ \vdots & \vdots & \ddots & \ddots & \vdots & \vdots \\ \bar{\beta}_2 & \bar{\beta}_3 & \cdots & \bar{\beta}_p & 1 & 0 \\ \bar{\beta}_1 & \bar{\beta}_2 & \cdots & \bar{\beta}_{p-1} & \bar{\beta}_p & 1 \end{bmatrix} \begin{bmatrix} 1 \\ \bar{k}_1 \\ \vdots \\ \bar{k}_{p-1} \\ \bar{k}_p \end{bmatrix} \quad (59)$$

So the state feedback gain $\bar{K}_o$ (34) and the observer gain $\bar{L}_o$ (33) can be solved numerically from Eqs.(58) and (59) if the numerator and denominator of the given controller $K_c(s)$ are available. However, the existence of the solution depends on the chosen numerical nonlinear equation solver and the initial guess. It is not always possible to solve the nonlinear equations (58) and (59).

A procedure will be proposed in this section to solve the problem. The procedure only involves finding the roots of polynomials, which is always possible for a polynomial with rational coefficients, thus it is guaranteed that solutions can be found for (58) and (59), thus the existence of a solution is guaranteed. The procedure depends on the following result.

Proposition: Denote the numerator and denominator polynomials of the feedback controller $C_2(s)$ of the pth-order SS-PID as $X(s)$ and $Y(s)$, respectively, i.e.,

$$C_2(s) = \frac{X(s)}{Y(s)} \quad (60)$$

Assume $Y(s)$ is monic, i.e., the coefficient of the highest term is unity. Then we have

$$s^p Y(s) + b_0 X(s) = M_{st}(s)M_{ob}(s) \quad (61)$$

where

$$M_{st}(s) = s^{p+1} + \bar{k}_1 s^p + \cdots + \bar{k}_p s + \bar{k}_{p+1} \quad (62)$$

is the characteristic polynomial of the state feedback law, and

$$M_{ob}(s) = s^p + \bar{\beta}_p s^{p-1} + \cdots + \bar{\beta}_2 s + \bar{\beta}_1 \quad (63)$$

is the characteristic polynomial of the observer.

Proof. It is observed that the pth-order SS-PID (29) is an observer-based state-feedback controller for the plant (32). So the closed-loop system for the plant (32) controlled by (29) with a negative feedback is then

$$\begin{cases} \dot{x} = \bar{A}_e x - \bar{B}_e\bar{K}_o\bar{x} \\ \dot{\bar{x}} = (\bar{A}_e - \bar{B}_e\bar{K}_o)\bar{x} + \bar{L}_o\bar{C}_e(x - \bar{x}) \end{cases} \quad (64)$$

Let

$$e = x - \bar{x} \tag{65}$$

then the closed-loop system becomes

$$\begin{pmatrix} \dot{e} \\ \dot{\bar{x}} \end{pmatrix} = \begin{bmatrix} \bar{A}_e - \bar{L}_o\bar{C}_e & 0 \\ \bar{L}_o\bar{C}_e & \bar{A}_e - \bar{B}_e\bar{K}_o \end{bmatrix} \begin{pmatrix} e \\ \bar{x} \end{pmatrix} \tag{66}$$

So the poles of the closed-loop system are determined by the eigenvalues of $\bar{A}_e - \bar{L}_o\bar{C}_e$ and $\bar{A}_e - \bar{B}_e\bar{K}_o$. The result is well-known for an observer-based state-feedback controller.

It is easy to verify that

$$\begin{aligned} &|sI - \bar{A}_e + \bar{B}_e\bar{K}_o| \\ &\quad = s^{p+1} + k_1 s^p + \cdots + k_p s + k_{p+1} = M_{st}(s) \end{aligned} \tag{67}$$

$$\begin{aligned} &|sI - \bar{A}_e + \bar{L}_o\bar{C}_e| \\ &\quad = s(s^p + \bar{\beta}_p s^{p-1} + \cdots + \bar{\beta}_2 s + \bar{\beta}_1) = sM_{ob}(s) \end{aligned} \tag{68}$$

So the poles of the closed-loop system for plant (32) controlled by (29) is composed of the roots of $M_{st}(s)$ and $M_{ob}(s)$, and $s = 0$ is canceled since it is a pole and a zero simultaneously.

Now if we consider the transfer function of the plant (32) and the feedback controller $C_2(s)$. Since the plant model is

$$P_m(s) = \frac{b_0}{s^p} \tag{69}$$

and the controller is

$$C_2(s) = \frac{X(s)}{Y(s)} \tag{70}$$

then the poles of the closed-loop system will be the zeros of $1 + P_m(s)C_2(s)$. Since

$$1 + P_m(s)C_2(s) = 1 + \frac{b_0}{s^p}\frac{X(s)}{Y(s)} = \frac{s^pY(s) + b_0X(s)}{s^pY(s)} \tag{71}$$

So if there are no pole-zero cancellation between $P_m(s)$ and $C_2(s)$, i.e., there are no zeros at the origin in $C_2(s)$, the zeros of $s^pY(s) + b_0X(s)$ will be equal to the poles of closed-loop system, i.e., the roots of $M_{st}(s)$ and $M_{ob}(s)$. Thus the proposition is proved.

This proposition relates the poles of the transfer function of the closed-loop system to the poles of the state-space realization of the closed-loop system. It is quite simple and straightforward. However, this proposition guarantees that any strictly-proper $(p+1)$th-order controller with integration can be realized with a fixed structure controller $C_2(s)$, or in other word, can be implemented as a feedback controller of a pth-order state-space PID (29).

The following gives the solution procedure. For any strictly-proper $(p+1)$th-order linear controller $K_c(s)$ with integration,

1) Find the numerator polynomial $X(s)$ and the denominator polynomial $Y(s)$ of $K_c(s)$. Let $Y(s)$ be monic.
2) Find the roots of the polynomial $s^pY(s) + b_0X(s)$ and denote them by m_i, $i = 1, \cdots, 2p+1$.
3) Divide the roots of $s^pY(s) + b_0X(s)$ into two groups, the first contains p roots $(m_1, \cdots, m_p)$ and the second has $p+1$ roots $(m_{p+1}, \cdots, m_{2p+1})$. Make sure that conjugate roots are grouped into the same group.
4) Form a polynomial with the first group of roots by $(s - m_1)\cdots(s - m_p)$ and expand the polynomial to get the coefficients.

$$(s - m_1)\cdots(s - m_p) = s^p + \bar{\beta}_p s^{p-1} + \cdots + \bar{\beta}_1 \tag{72}$$

Then

$$\bar{L}_o = [\bar{\beta}_1 \;\; \bar{\beta}_2 \;\; \cdots \;\; \bar{\beta}_p \;\; 1]^T / b_0 \tag{73}$$

5) Form a polynomial with the second group of roots by $(s - m_{p+1})\cdots(s - m_{2p+1})$ and expand the polynomial to get the coefficients.

$$\begin{aligned} &(s - m_{p+1})\cdots(s - m_{2p+1}) \\ &\qquad = s^{p+1} + \bar{k}_1 s^p + \cdots + \bar{k}_p s + \bar{k}_{p+1} \end{aligned} \tag{74}$$

Then

$$\bar{K}_o = [\bar{k}_1 \;\; \cdots \;\; \bar{k}_p \;\; \bar{k}_{p+1}] \tag{75}$$

With the parameters b_0, $\bar{K}_o$, and $\bar{L}_o$, the feedback controller $C_2(s)$ of the SS-PID (29) is exactly equal to $K_c(s)$.

Example 3: Consider the PID controller (28) discussed in Example 1. To reduce the effect of noise in the measurement, a second-order filter is usually used together with the ideal PID, i.e., the controller is of the following form (hereafter referred as **PIDF** controller).

$$K_c(s) = K_p\left(1 + \frac{1}{T_i s} + T_d s\right)\frac{1}{T_f^2 s^2/2 + T_f s + 1} \tag{76}$$

T_f is chosen as $T_f = 0.22T_d$ as recommended in [21].

The PIDF is a third-order strictly-proper controller with integration, thus can be implemented with a second-order SS-PID. Let $b_0 = 1$. Follow the proposed procedure, the roots of $s^2Y(s) + b_0X(s)$ are

$$\begin{aligned} p_{1,2} &= -25.3609 \pm 25.3363j, \quad p_3 = -0.9064 \\ p_{4,5} &= 0.3596 \pm 1.3379j \end{aligned} \tag{77}$$

Choose the first two roots p_1, p_2 as the roots of $M_{ob}(s)$ and the last three roots p_3, p_4, p_5 as the roots of $M_{st}(s)$, then we get a second-order SS-PID with gains:

$$\begin{aligned} \bar{L}_o &= [1285.105 \;\; 50.722 \;\; 1]^T \\ \bar{K}_o &= [0.1872 \;\; 1.2674 \;\; 1.7397] \end{aligned} \tag{78}$$

It is easy to verify that solution (78) satisfy (56).

Figure 7 shows the responses of the plant (27) under the control of the PIDF controller (76) and the SS-PID (78) with a step setpoint at $t = 1$s and a step input disturbance at $t = 10$s. It is shown that the SS-PID (78) has the same disturbance rejection responses as the PIDF controller (76) as expected, but they have different setpoint and initial controller responses.

Remark 6: It is shown that any linear finite-dimensional strictly-proper controller with integration can be implemented via the SS-PID structure, thus it can serve as a

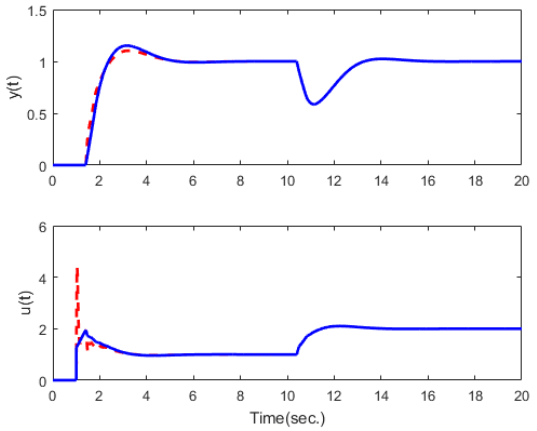

FIGURE 7. Responses for Example 3 (solid: second-order SS-PID (78); dashed: PIDF controller with parameter (28)).

general-purposed linear control structure that has a fixed structure and only parameters are needed to tune to meet the desired control performance. If a linear strictly-proper controller has already been designed by another linear control method, it can be implemented using the SS-PID structure via the proposed procedure. In other words, any linear strictly-proper controller with integration is a (high-order) 'PID' controller. State-space PID is thus a control structure that fills the gap between classical and modern control theory.

VI. STATE-SPACE PID DESIGN

Any PID design or tuning method can be used to get the parameters of an ideal PID, and then an observer (13) can be used to get the state-space PID. State feedback design is a convenient and useful control design method in modern control theory. Is it possible to apply the state feedback design in PID design? The extended model (32) can be used to design a PID controller, however, since the internal dynamic information of the controlled plant is not used in design, it cannot guarantee the stability of the actual plant. Model information may be used to design a stabilizing PID control.

Suppose the controlled plant has a minimal state-space realization as follows:

$$\begin{cases} \dot{x}_m = A_m x_m + B_m u \\ y = C_m x \end{cases} \tag{79}$$

A state feedback control law $u = K_m x_m$ can be obtained using well-known pole-placement method. However, since the state vector x_m is not necessarily composed of y and its derivatives, thus K_m is not a PID control gain. To solve the problem, consider the observable canonical form of the controlled plant:

$$\begin{cases} \dot{\xi} = A_o \xi + B_o u \\ y = C_o \xi \end{cases} \tag{80}$$

where $\xi = [\xi_1 \ \ \xi_2 \ \ \cdots \ \ \xi_p]^T$ is the state vector, and

$$A_o = \begin{bmatrix} 0 & 1 & 0 & \cdots & 0 \\ 0 & 0 & 1 & \cdots & 0 \\ \vdots & \vdots & \vdots & \ddots & \vdots \\ 0 & 0 & 0 & \cdots & 1 \\ -a_0 & -a_1 & -a_2 & \cdots & -a_{p-1} \end{bmatrix}, \quad B_o = \begin{bmatrix} d_1 \\ d_2 \\ d_3 \\ \vdots \\ d_p \end{bmatrix},$$
$$C_o = \begin{bmatrix} 1 & 0 & \cdots & 0 & 0 \end{bmatrix} \tag{81}$$

The state transformation matrix is T_o, where T_o is the observability matrix of (79), and

$$A_o = T_o A_m T_o^{-1}, \quad B_o = T_o B_m, \ C_o = C_m T_o^{-1} \tag{82}$$

In this canonical form, the elements of the state vector ξ are related by

$$\begin{aligned} \dot{\xi}_1 &= \xi_2 + d_1 u \\ \dot{\xi}_2 &= \xi_3 + d_2 u \\ &\vdots \\ \dot{\xi}_{p-1} &= \xi_n + d_{p-1} u \end{aligned} \tag{83}$$

Since $y = \xi_1$, we have

$$\begin{aligned} \xi_2 &= \dot{\xi}_1 - d_1 u = \dot{y} - d_1 u \\ \xi_3 &= \dot{\xi}_2 - d_2 u = \ddot{y} - d_1 \dot{u} - d_2 u \\ &\vdots \\ \xi_p &= \dot{\xi}_{p-1} - d_{p-1} u \\ &= y^{(p-1)} - d_1 u^{(p-2)} - \cdots - d_{p-1} u \end{aligned} \tag{84}$$

Define a new state as

$$\dot{\xi}_{p+1} = \xi_1 = y \tag{85}$$

so ξ_{p+1} is the integral of y, and the extended state-space model of the controlled plant is

$$\begin{cases} \begin{bmatrix} \dot{\xi} \\ \dot{\xi}_{p+1} \end{bmatrix} = \begin{bmatrix} A_o & 0 \\ C_o & 0 \end{bmatrix} \begin{bmatrix} \xi \\ \xi_{p+1} \end{bmatrix} + \begin{bmatrix} B_o \\ 0 \end{bmatrix} u \\ y = \begin{bmatrix} C_o & 0 \end{bmatrix} \begin{bmatrix} \xi \\ \xi_{p+1} \end{bmatrix} \end{cases} \tag{86}$$

Suppose a state-feedback control law has been designed for (86):

$$\begin{aligned} u &= k_1 \xi_1 + k_2 \xi_2 + \cdots + k_p \xi_p + k_{p+1} \xi_{p+1} \\ &= k_1 y + k_2 (\dot{y} - d_1 u) + \cdots \\ &\quad + k_p (y^{(n-1)} - d_1 u^{(p-2)} - \cdots - d_{p-1} u) \\ &\quad + k_{p+1} \int_0^t y(\tau) d\tau \end{aligned} \tag{87}$$

Ignore the derivatives of u, we have

$$u = \frac{k_1 y + k_2 \dot{y} + \cdots + k_p y^{(p-1)} + k_{p+1} \int_0^t y(\tau) d\tau}{1 + \sum_{i=2}^{p} k_i d_{i-1}} \tag{88}$$

So u is a combination of the derivatives and integral of y, a high-order PID control. For second-order system ($p = 2$), (88) is the classical PID control, with

$$K_p = \frac{k_1}{1 + k_2 d_1}, \quad K_i = \frac{k_3}{1 + k_2 d_1}, \; K_d = \frac{k_2}{1 + k_2 d_1} \tag{89}$$

For third-order system ($p = 3$), (88) is PIDD^2, with

$$\begin{aligned} K_p &= \frac{k_1}{1 + k_2 d_1 + k_3 d_2}, \quad K_i = \frac{k_4}{1 + k_2 d_1 + k_3 d_2}, \\ K_{d1} &= \frac{k_2}{1 + k_2 d_1 + k_3 d_2}, \quad K_{d2} = \frac{k_3}{1 + k_2 d_1 + k_3 d_2} \end{aligned} \tag{90}$$

The state-feedback law (87) can be designed by the well-known pole-placement method. For simplicity, the poles can be chosen as:

$$s_{1,2} = -\bar{\omega}_c(\bar{\zeta} \pm \sqrt{1 - \bar{\zeta}^2} j), \quad s_i = -\bar{\alpha}\bar{\omega}_c (i = 3, \cdots, p) \tag{91}$$

From extensive simulations, the damping ratio ($\bar{\zeta}$) of the dominant poles can be chosen as 0.8 and $\bar{\alpha}$ can be chosen as 2 for other poles so that the disturbance rejection response has good damping and fast settling time. So we need only one parameter $\bar{\omega}_c$ to tune $\bar{K}_o$ (34) and one parameter $\bar{\omega}_o$ to tune $\bar{L}_o$ (33) with

$$\beta_i = C_p^{i-1} \bar{\omega}_o^{p-i+1} \quad (i = 1, \cdots, p) \tag{92}$$

For processes with time delay, delay can be approximated using first-order Pade approximation. The following examples show that this approximation is good enough for the design of state-space PID.

Example 4: Consider the FOPDT plant (27) in Example 1. To tune a state-space PID for this plant, choose $\bar{\omega}_c = 1.8$ and we get a PID with the following gains:

$$K_p = 1.6082, \quad K_i = 1.9085, \; K_d = 0.1819 \tag{93}$$

With $\bar{\omega}_o = 20$ we get a second-order SS-PID with the following gains:

$$\begin{aligned} \bar{K}_o &= [0.1819 \;\; 1.6082 \;\; 1.9085], \\ \bar{L}_o &= [400 \;\; 40 \;\; 1]^T, \quad b_0 = 1 \end{aligned} \tag{94}$$

Figure 8(a) shows the responses of the plant (27) under the control of the SS-PID controller (94) with a step setpoint at $t = 1$s and a step input disturbance at $t = 10$s. For comparison, the responses of the PIDF controllers with $T_f = 0.22T_d$ are also shown in the figure. The parameters of the two PIDF controllers are from (93) and (28). It is shown that the SS-PID (94) has almost the same disturbance rejection responses as the PIDF controller with parameter (93) (indistinguishable in the figure), and better disturbance rejection than the PIDF controller with parameter (28). The total variations ($TV = \sum_1^\infty |u_{i+1} - u_i|$) of the control input $u(t)$ for the SS-PID (94), the PIDF with (93) and (28) are 4.8155, 13.2344, and 11.2804, respectively, so the SS-PID (94) has the smallest TV thus has the best control effort [45].

The Bode plots for the feedback controllers $C_2(s)$ of the SS-PID (78), the PIDF controllers with parameters (93) and (28) are shown in Figure 8(b). It is clear that all the three controllers roll off at high frequencies thus can attenuate measurement noise as expected. The SS-PID (94) has the largest roll-off rate thus the SS-PID has the best performance against high-frequency noise.

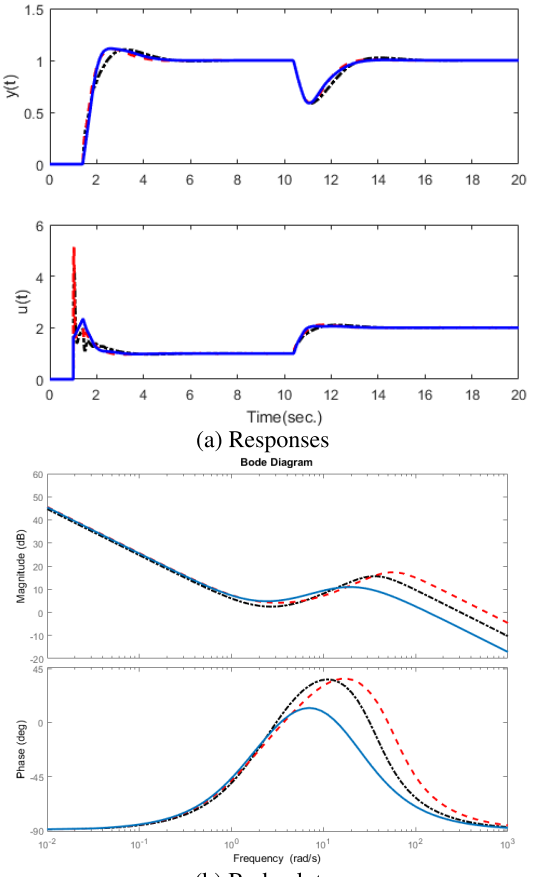

(a) Responses

(b) Bode plots

FIGURE 8. Responses and bode plots of various PID for Example 4 (solid: SS-PID (94); dashed: PIDF (93); dashdotted: PIDF (28)).

The proposed method is not only suitable for stable processes but also for integrating and unstable processes.

Example 5: Consider an unstable plant with large time delay

$$P_2(s) = \frac{1}{s - 1} e^{-1.2s} \tag{95}$$

It is very difficult to control with a PID controller considering the instability property and the large time delay. A modified internal model control (IMC) control structure is designed in [46] with

$$K_0 = 2, \quad K_1 = \frac{s + 1}{2s + 1}, \; K_2 = 1.1(1 + 0.49s) \tag{96}$$

and a PID+lead controller is designed in [26] with

$$\begin{aligned} K &= 0.0317(1 + \frac{1}{0.8s} + 0.3s)\frac{29.7476s + 1}{0.2709s + 1}, \\ f_R &= \frac{1}{29.7476s + 1} \end{aligned} \tag{97}$$

where f_R is the setpoint filter.

To tune a state-space PID for this plant, choose $\bar{\omega}_c = 0.42$ and we get a PID with the following gains:

$$K_p = 1.1806, \quad K_i = 0.0322, \; K_d = 0.6373 \tag{98}$$

The extended observer gain can be tuned with the observer bandwidth $\bar{\omega}_o = 50$, thus a second-order SS-PID with the following parameters can be obtained:

$$\begin{aligned} \bar{K}_o &= [0.6373 \;\; 1.1806 \;\; 0.0322], \quad b_0 = 1 \\ \bar{L}_o &= [2500 \;\; 100 \;\; 1]^T, \quad \alpha = 0.05 \end{aligned} \tag{99}$$

Here a setpoint weight $\alpha = 0.05$ is used to reduce the large overshoot of the setpoint response.

Figure 9 shows the responses of the plant (95) under the control of the SS-PID controller (99), PID+lead controller (97), and modified IMC (96) with a step setpoint at $t = 1$s and a step input disturbance at $t = 40$s. It is shown that the SS-PID (99) has almost the same disturbance rejection responses as the modified IMC controller. Though the disturbance rejection response of the PID+lead controller is the best among the three controllers, however, the controller response is oscillatory. In fact, the PID+lead controller (97) is not internally stable for plant (95) though the response is stable within the simulation period. However, as the simulation time becomes longer, the response will become unstable. The total variations of the control input $u(t)$ for the SS-PID (99) and the modified IMC are 3.27 and 3.70, respectively, so the SS-PID (99) has better control effort.

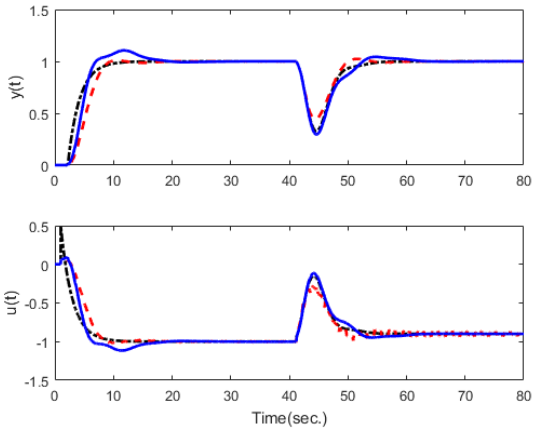

FIGURE 9. Responses of various controllers for Example 5 (solid: SS-PID (99); dashed: PID+lead (97); dashdotted: modified IMC (96)).

The next example shows that a high-order PID can achieve better performance than a classical PID.

Example 6: Consider an integrating plant with non-minimum phase zero

$$P_3(s) = \frac{-0.2s + 1}{s(s-1)} e^{-0.2s} \tag{100}$$

A PID controller is designed in [47] with

$$\begin{aligned} K &= 0.4451(1 + \frac{1}{5.218s} + 4.33s), \\ f_R &= \frac{1.3s + 1}{21.9s^2 + 5.0833s + 1} \end{aligned} \tag{101}$$

where f_R is the setpoint filter.

To tune a state-space PID for this plant, choose $\bar{\omega}_c = 0.8$ and we get a PIDD^2 controller with the following gains:

$$K_p = 0.5742, \quad K_i = 0.1618, \; K_d = 1.8894, \; K_{d2} = 0.0814 \tag{102}$$

The extended observer gain can be tuned with the observer bandwidth $\bar{\omega}_o = 15$, thus a second-order SS-PID with the following parameters can be obtained:

$$\begin{aligned} \bar{K}_o &= [0.0814 \;\; 1.8894 \;\; 0.5742 \;\; 0.1618], \quad b_0 = 1 \\ \bar{L}_o &= [3375 \;\; 675 \;\; 45 \;\; 1]^T, \quad \alpha = 0 \end{aligned} \tag{103}$$

Figure 10 shows the responses of the plant (100) under the control of the SS-PID controller (103) and the PID controller (101) with a step setpoint at $t = 1$s and a step input disturbance with magnitude 0.5 at $t = 30$s. It is shown that the SS-PID (103) has much better disturbance rejection response than the PID controller (101). The total variations of the control input $u(t)$ for the SS-PID (103) and the PID (101) are 4.48 and 5.73, respectively, so the SS-PID (103) has better control effort.

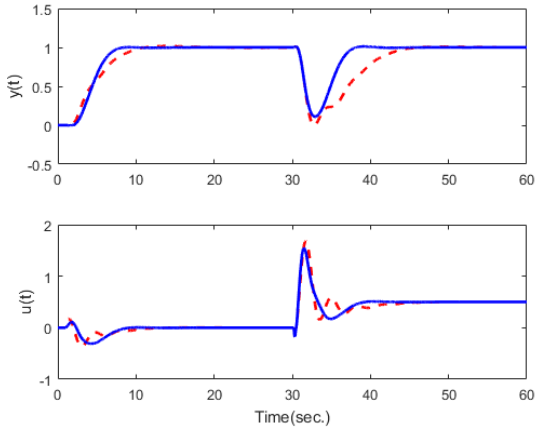

FIGURE 10. Responses of various controllers for Example 6 (solid: SS-PID (103); dashed: PID (101)).

VII. EXPERIMENT VALIDATION

Consider the temperature control lab (TClab) [48] shown in Figure 11. The temperature control lab is an application of feedback control with an Arduino, an LED, two heaters, and two temperature sensors. The heater power output (mV) is adjusted to maintain a desired temperature setpoint ($^\circ C$). Thermal energy from the heater is transferred by conduction, convection, and radiation to the temperature sensor. TCLab, as a hardware benchmark device, is widely used in process control teaching. The Arduino microcontroller is

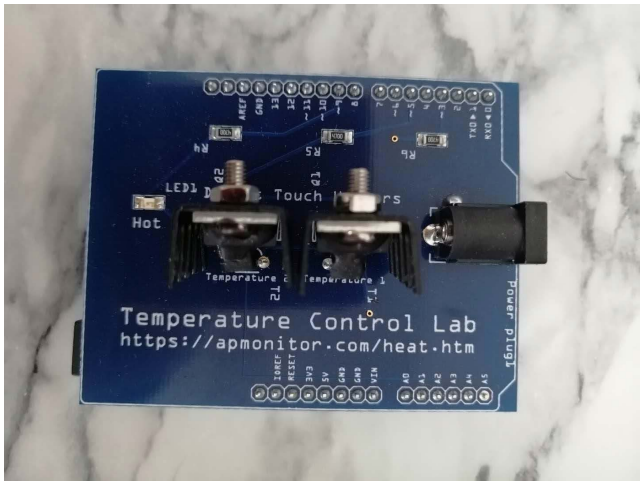

FIGURE 11. Temperature control lab.

programmed in advance as a safety measure to turn off the heater when the temperature exceeds $100°C$. The difficulty of this experiment is that it is easily affected by the noisy environment, such as ambient temperature, power output and airflow (near the computer fan), and the controller is quite sensitive to the noise.

Consider the single heater case. A first-order plus deadtime (FOPDT) model can be identified from the step response of the temperature control system [49] as:

$$P(s) = \frac{0.836}{161.3s + 1} e^{-23.4s} \tag{104}$$

An ideal PID controller for the temperature control system can be designed via the proposed pole-placement method with $\bar{\omega}_c = 0.025$.

$$K_p = 4.685, \quad K_i = 0.0615, \; K_d = 24.8635 \tag{105}$$

The ideal PID can be implemented with the proposed SS-PID (29) with parameters

$$\begin{aligned} b_0 &= 0.0001, \quad \bar{K}_o = [24.8635 \;\; 4.685 \;\; 0.0615]b_0, \\ \bar{L}_o &= [0.09 \;\; 0.6 \;\; 1]^T / b_0 \end{aligned} \tag{106}$$

and a second-order LADRC (48) is implemented with the following parameters (dual of SS-PID)

$$\begin{aligned} b_0 &= 0.0001, \quad \hat{K}_o = [0.09 \;\; 0.6 \;\; 1]/b_0 \\ \hat{L}_o &= [24.8635 \;\; 4.685 \;\; 0.0615]^T b_0 \end{aligned} \tag{107}$$

Figure 12 shows the Bode plots of the feedback controller of the SS-PID (106), the ideal PID (105) and its practical form (23) with ($N = 20$). It is shown that the SS-PID approximates the ideal PID up to frequency 0.2rad/s and then rolls off at the high frequency. The Bode plot of the second-order LADRC (107) is the same as that of the SS-PID (105) thus not shown in the figure. Compared with the practical PID, the proposed SS-PID has a larger roll-off rate thus will be more insensitive to noise.

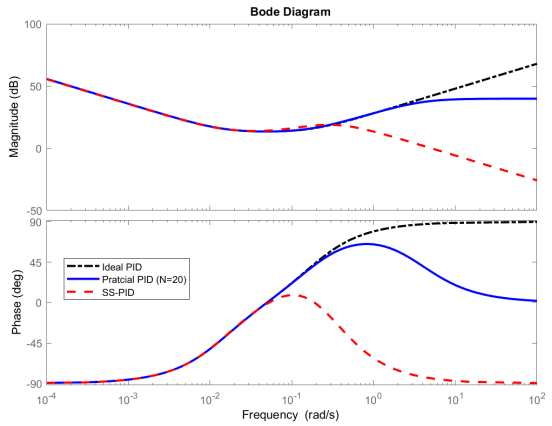

FIGURE 12. Bode plots of various PID for TClab.

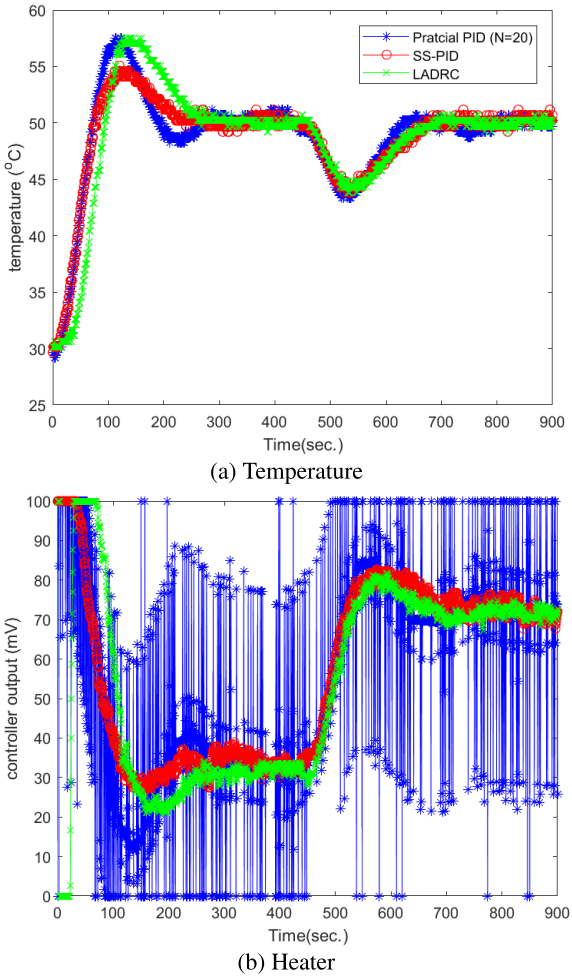

FIGURE 13. Responses of the temperature control lab (solid: SS-PID; dashed: LADRC; dash-dotted: practical PID).

Figure 13 shows the responses of the proposed SS-PID (106), the LADRC (107), and the practical PID when there is a step temperature setpoint change at $t = 0$s from $30°C$ to $50°C$ and a step input disturbance of magnitude 40 at $t = 450$s. The SS-PID has similar response as the practical PID, but the SS-PID has smaller initial and

smoother controller output compared with the practical PID. The controller output of the practical PID oscillates rapidly between 0 (minimum) and 100 (maximum). The disturbance response of the LADRC is similar to that of the SS-PID (they should be the same without noise) but the tracking responses are different. The total variants (TV) of the control input $u(t)$ for the SS-PID, the LADRC, and the practical PID are 831.8, 968.5, and 35875, respectively, so the SS-PID has the best control effort.

VIII. CONCLUSION

A state-space PID control structure was proposed to implement the ideal PID. The state-space PID adopts a cascaded integral model to estimate the plant output and its derivatives, thus it retains the model-independence property of the classical PID. Compared with the PID control, a state-space PID has roll-off at high frequencies thus it is more insensitive to measurement noise. The state-space PID idea was also extended to high-order cases, and it was shown that the state-space PID structure is a general-purposed control structure in that any linear finite-dimensional strictly-proper controller with integration can be implemented with the structure. A state feedback pole-placement method was proposed to design the PID gains and thus the state-space PID can be tuned with two parameters. Simulation and experiment results showed that state-space PID is a practical implementation of the ideal PID with roll-off at high frequencies, thus measurement noise can be simultaneously considered in PID tuning.

It is interesting to observe that the proposed state-space PID structure is the dual of LADRC structure, and they both use the same canonical model in controller design. The difference is that state-space PID extends the model with the integral of the output as the extended state and LADRC extends the model with the total disturbance as the extended state. In the future research the two design methods will be further investigated and the relationship between the state-space PID and the LQG and H_∞ controllers will be investigated to fill the gap between PID and modern control.

REFERENCES

[1] K. J. Astrom and H. Hagglund, *PID Controllers: Theory, Design, and Tuning*, 2nd ed. Research Triangle Park, NC, USA: Instrument Society of America, 1995.
[2] K. H. Ang, G. Chong, and Y. Li, "PID control system analysis, design, and technology," *IEEE Trans. Control Syst. Technol.*, vol. 13, no. 4, pp. 559–576, Jul. 2005.
[3] R. Vilanova and A. Visioli, *PID Control in the Third Millennium*. London, U.K.: Springer, 2012.
[4] S. W. Sung and I.-B. Lee, "Limitations and countermeasures of PID controllers," *Ind. Eng. Chem. Res.*, vol. 35, no. 8, pp. 2596–2610, Jan. 1996.
[5] K. J. Astrom, *Introduction to Stochastic Control Theory*. Boston, MA, USA: Academic, 1970.
[6] K. Zhou and J. C. Doyle, *Essentials of Robust Control*. Upper Saddle River, NJ, USA: Prentice-Hall, 1998.
[7] K. J. Astrom and B. Wittenmark, *Adaptive Control*. Reading, MA, USA: Addison-Wesley, 1995.
[8] K. J. Åström and T. Hågglund, "The future of PID control," *Control Eng. Pract.*, vol. 9, pp. 1163–1175, Feb. 2001.
[9] J. G. Ziegler and N. B. Nichols, "Optimum settings for automatic controllers," *Trans. ASME*, vol. 62, pp. 759–768, Nov. 1942.
[10] K. J. Åström and T. Hägglund, "Automatic tuning of simple regulators with specifications on phase and amplitude margins," *Automatica*, vol. 20, no. 5, pp. 645–651, 1984.
[11] W. K. Ho, O. P. Gan, E. B. Tay, and E. L. Ang, "Performance and gain and phase margins of well-known PID tuning formulas," *IEEE Trans. Control Syst. Technol.*, vol. 4, no. 4, pp. 473–477, Jul. 1996.
[12] D. E. Rivera, M. Morari, and S. Skogestad, "Internal model control: PID controller design," *Ind. Eng. Chem. Process Des. Dev.*, vol. 25, pp. 252–265, Jan. 1986.
[13] Y. Lee, S. Park, M. Lee, and C. Brosilow, "PID controller tuning for desired closed-loop responses for Si/SO systems," *AIChE J.*, vol. 44, no. 1, pp. 106–115, Jan. 1998.
[14] Q. Wang, C. Lu, and W. Pan, "IMC PID controller tuning for stable and unstable processes with time delay," *Chem. Eng. Res. Des.*, vol. 45, pp. 43–54, Jan. 2016.
[15] G. J. Silva, A. Datta, and S. P. Bhattacharyya, "Stabilization of first-order systems with time delay using the PID controller," in *Proc. Amer. Control Conf.*, Arlington, VA, USA, 2001, pp. 4650–4655.
[16] D. Chen and D. E. Seborg, "PI/PID controller design based on direct synthesis and disturbance rejection," *Ind. Eng. Chem. Res.*, vol. 41, no. 19, pp. 4807–4822, Sep. 2002.
[17] R. C. Panda, "Synthesis of PID controller for unstable and integrating processes," *Chem. Eng. Sci.*, vol. 64, no. 12, pp. 2807–2816, Jun. 2009.
[18] H.-P. Huang, J.-C. Jeng, and K.-Y. Luo, "Auto-tune system using single-run relay feedback test and model-based controller design," *J. Process Control*, vol. 15, no. 6, pp. 713–727, Sep. 2005.
[19] R. P. Borase, D. K. Maghade, S. Y. Sondkar, and S. Y. Pawar, "A review of PID control, tuning methods and applications," *Int. J. Dyn. Control*, vol. 9, pp. 818–827, Jul. 2021.
[20] A. J. Isaksson and S. F. Graebe, "Derivative filter is an integral part of PID design," *IEE Proc. Control Theory Appl.*, vol. 149, no. 1, pp. 41–45, Jan. 2002.
[21] V. R. Segovia, T. Hagglund, and K. J. Astrom, "Measurement noise filtering for PID controllers," *J. Process Control*, vol. 24, no. 4, pp. 299–313, 2014.
[22] V. R. Segovia, T. Hägglund, and K. J. Åström, "Measurement noise filtering for common PID tuning rules," *Control Eng. Pract.*, vol. 32, pp. 43–63, Nov. 2014.
[23] A. D. Micić and M. R. Mataušek, "Optimization of PID controller with higher-order noise filter," *J. Process Control*, vol. 24, no. 5, pp. 694–700, May 2014.
[24] O. Garpinger and T. Hägglund, "Software-based optimal PID design with robustness and noise sensitivity constraints," *J. Process Control*, vol. 33, pp. 90–101, Sep. 2015.
[25] M. Shamsuzzoha and M. Lee, "Design of advanced PID controller for enhanced disturbance rejection of second-order processes with time delay," *AIChE J.*, vol. 54, no. 6, pp. 1526–1536, 2008.
[26] M. Shamsuzzoha and M. Lee, "Analytical design of enhanced PID filter controller for integrating and first order unstable processes with time delay," *Chem. Eng. Sci.*, vol. 63, no. 10, pp. 2717–2731, May 2008.
[27] M. Shamsuzzoha and M. Lee, "Enhanced disturbance rejection for open-loop unstable process with time delay," *ISA Trans.*, vol. 48, no. 2, pp. 237–244, Apr. 2009.
[28] B. M. Vinagre, C. A. Monje, A. J. Calderón, and J. I. Suárez, "Fractional PID controllers for industry application. A brief introduction," *J. Vib. Control*, vol. 13, nos. 9–10, pp. 1419–1429, Sep. 2007.
[29] A. Soukkou, M. C. Belhour, and S. Leulmi, "Review, design, optimization and stability analysis of fractional-order PID controller," *Int. J. Intell. Syst. Technol. Appl.*, vol. 8, no. 7, pp. 73–96, Jul. 2016.
[30] M. Ge, M.-S. Chiu, and Q.-G. Wang, "Robust PID controller design via LMI approach," *J. Process Control*, vol. 12, no. 1, pp. 3–13, 2002.
[31] F. Zheng, Q.-G. Wang, and T. H. Lee, "On the design of multivariable PID controllers via LMI approach," *Automatica*, vol. 38, no. 3, pp. 517–526, Mar. 2002.
[32] J. Han, "From PID to active disturbance rejection control," *IEEE Trans. Ind. Electron.*, vol. 56, no. 3, pp. 900–906, Mar. 2009.
[33] Z. Gao, "Scaling and bandwidth-parameterization based controller tuning," in *Proc. Amer. Control Conf.*, Denver, CO, USA, 2003, pp. 4989–4996, doi: 10.1109/ACC.2003.1242516.
[34] Z. Gao, "Active disturbance rejection control: A paradigm shift in feedback control system design," in *Proc. IEEE Amer. Control Conf.*, Minneapolis, MN, USA, Jun. 2006, pp. 2399–2405.

[35] H. Jin, J. Song, W. Lan, and Z. Gao, "On the characteristics of ADRC: A PID interpretation," *Sci. China Inf. Sci.*, vol. 63, no. 10, Oct. 2020, Art. no. 209201.
[36] C. Zhao and D. Li, "Control design for the SISO system with the unknown order and the unknown relative degree," *ISA Trans.*, vol. 53, no. 4, pp. 858–872, Jul. 2014.
[37] R. Zhou, W. Han, and W. Tan, "On applicability and tuning of linear active disturbance rejection control," *Control Theory Appl.*, vol. 35, no. 11, pp. 1654–1662, 2018.
[38] Z. Nie, Z. Li, Q. Wang, Z. Gao, and J. Luo, "A unifying Ziegler–Nichols tuning method based on active disturbance rejection," *Int. J. Robust Nonlinear Control*, vol. 31, pp. 1–17, Oct. 2021, doi: 10.1002/rnc.5848.
[39] W.-H. Chen, J. Yang, L. Guo, and S. Li, "Disturbance-observer-based control and related methods—An overview," *IEEE Trans. Ind. Electron.*, vol. 63, no. 22, pp. 1083–1095, Feb. 2015.
[40] F. Esfandiari and H. K. Khalil, "Output feedback stabilization of fully linearizable systems," *Int. J. Control*, vol. 56, no. 5, pp. 1007–1037, 1992.
[41] J. Doyle and G. Stein, "Robustness with observers," *IEEE Trans. Autom. Control*, vol. AC-24, no. 4, pp. 607–611, Aug. 1979.
[42] J. B. He, Q. G. Wang, and T. H. Lee, "PI/PD controller tuning via LQR approach," *Chem. Eng. Sci.*, vol. 55, no. 13, pp. 2429–2439, 2000.
[43] K. J. Åström and T. Hägglund, "Revisiting the Ziegler–Nichols step response method for PID control," *J. Process Control*, vol. 14, no. 6, pp. 635–650, Sep. 2004.
[44] W. Tan and C. Fu, "Linear active disturbance-rejection control: Analysis and tuning via IMC," *IEEE Trans. Ind. Electron.*, vol. 63, no. 4, pp. 2350–2359, Apr. 2016.
[45] S. Skogestad, "Simple analytic rules for model reduction and PID controller tuning," *J. Process Control*, vol. 13, no. 4, pp. 291–309, Jun. 2003.
[46] W. Tan, H. J. Marquez, and T. Chen, "IMC design for unstable processes with time delays," *J. Process Control*, vol. 13, no. 3, pp. 203–213, Apr. 2003.
[47] K. G. Begum, A. S. Rao, and T. K. Radhakrishnan, "Enhanced IMC based PID controller design for non-minimum phase (NMP) integrating processes with time delays," *ISA Trans.*, vol. 68, pp. 223–234, May 2017.
[48] J. Park, R. A. Martin, J. D. Kelly, and J. D. Hedengren, "Benchmark temperature microcontroller for process dynamics and control," *Comput. Chem. Eng.*, vol. 135, Apr. 2020, Art. no. 106736.
[49] B. Zhang, W. Tan, and J. Li, "Tuning of linear active disturbance rejection controller with robustness specification," *ISA Trans.*, vol. 85, pp. 237–246, Feb. 2019.

WEN TAN (Member, IEEE) received the B.Sc. degree in applied mathematics and the M.Sc. degree in systems science from Xiamen University, Xiamen, China, in 1990 and 1993, respectively, and the Ph.D. degree in automation from the South China University of Technology, Guangzhou, China, in 1996. In 1996, he joined as a Faculty Member with the Power Engineering Department, North China Electric Power University, China. From January 2000 to December 2001, he was a Postdoctoral Fellow with the Department of Electrical and Computer Engineering, University of Alberta, Canada. He is currently a Professor with the School of Electrical and Control Engineering, North China University of Technology, China. His research interests include modeling, analysis, and control of complex industrial processes.

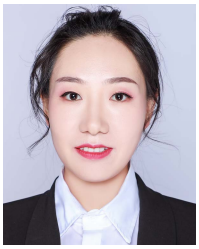

WENJIE HAN received the B.S. degree in wind energy and power engineering from the Hebei University of Architecture, Zhangjiakou, China, in 2016, and the M.S. degree in control theory and control engineering from North China Electric Power University, Beijing, China, in 2019, where she is currently pursuing the Ph.D. degree in control science and engineering. Her research interest includes advanced control theory and its applications in power systems.

JIAOHU XU received the B.S. and M.S. degrees in computer application technology from North China Electric Power University, Beijing, China, in 1998 and 2004, respectively. In 2004, he joined as a Faculty Member with the School of Control and Computer Engineering, North China Electric Power University. He is currently a Research Fellow with the Laboratory Teaching Center. His research interests include power system operation and control and artificial intelligence.